The testing of end fillet welds

Autor(en): **Eb, W.J. van der**

Objekttyp: **Article**

Zeitschrift: **IABSE congress report = Rapport du congrès AIPC = IVBH Kongressbericht**

Band (Jahr): **4 (1952)**

PDF erstellt am: **22.07.2024**

Persistenter Link: https://doi.org/10.5169/seals-5044

BI 2

The testing of end fillet welds

L'examen de soudures angulaires frontales

Die Prüfung von elektrisch geschweissten Stirnkehlnähten

IR. W. J. VAN DER EB
Research Engineer, T.N.O., Delft, Holland

INTRODUCTION

The tests were planned in such a way that a large series of end fillet welds are loaded till rupture by a force working at a predetermined angle α with the narrowest cross-section of the weld, in this paper called "neck section." Adjusting the apparatus it is possible to vary this angle α to obtain various combinations of stresses. The testing apparatus designed for this purpose is an improved construction of the apparatus already employed by C. D. Jenssen and Prof. Ir. N. C. Kist. The aim was to construct an apparatus of such a kind that in the first place the test pieces can be changed in as easy a manner as possible, while in the second place the largest possible range of stress combinations is obtainable. These stress combinations may be divided into three main categories:

(1) A predominantly tensile component combined with a smaller shearing component (fig. I[a]).
(2) A predominantly shearing component combined with a smaller tensile or compression component (fig. I[b]).
(3) A predominantly compression component with a smaller shearing component (fig. I[c]).

The apparatus designed by Engrs. Zwart and Louw is shown in principle in figs. 1 and 2. It will be seen that the apparatus and the action of the forces exerted upon it are based on the principle of "yielding of the end fillet weld." This yielding is soon achieved in a very expeditious manner by the presence of a sharp notch in the end fillet weld. When the triangle forming the weld yields at every part the force K acting upon that triangle can be conceived in a simple manner as a force passing through the axis of the neck section, so that the whole system thus becomes statically determinate. The magnitude and direction of the force K are defined by the variable distance a, the dimensions of the instrument and the magnitude of the force P exerted on the compression machine and indicated on the dial of the manometer. The

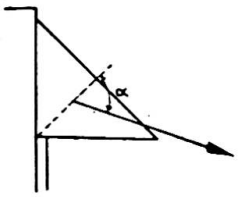

Fig. I

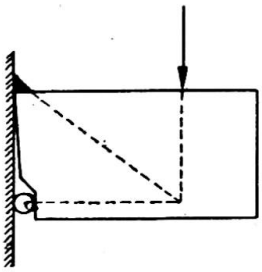

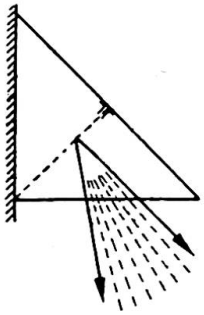

Fig. I[a]

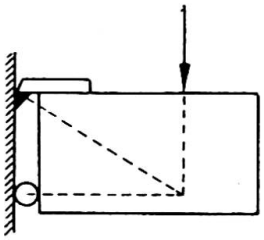

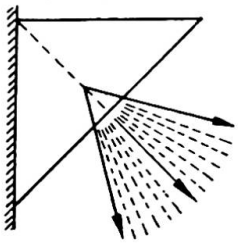

Fig. I[b]

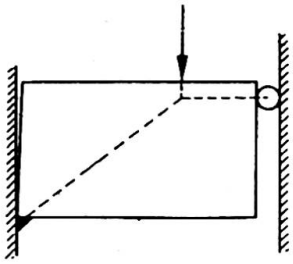

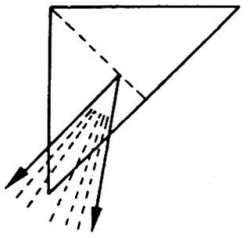

Fig. I[c]

variable distance a also serves for varying the angle α. Readings were taken of the applied forces and of the degree of deformation, by means of dial gauges shown in figs. 3 and 4. These dial gauges operate on a steel rule that is rigidly fixed on block A to which force P is applied.

The purpose of the deformation measurement was to find a definite yield point of the end fillet weld if such a yield point exists. Figs. 3 and 4 also show the situation during test, carried out with the aid of the pulsator in the Metallographic Laboratory of Prof. Brandsma in Delft.

A measuring process was exerted whereby the force P increases at a uniform rate, the dial gauges being read while P attained certain predetermined ascending values up to rupture. The lines of deformation as a function of the stress were plotted graphically in each case. It was not found possible to establish a distinct yield point

such as is found in the case of a linear stress condition with unobstructed elongation. It was noticed that in certain ranges near the point of rupture there was no longer a linear relation between stress and strain.

Fig. 5 shows the result of the rupture stresses, measured with respect to the neck section, plotted in a polar diagram. It will be seen that at some places the amount of dispersion in the results is considerable. Fig. 6 also shows the average result of all the readings.

The test showed, furthermore, that the neck section cannot in general be regarded

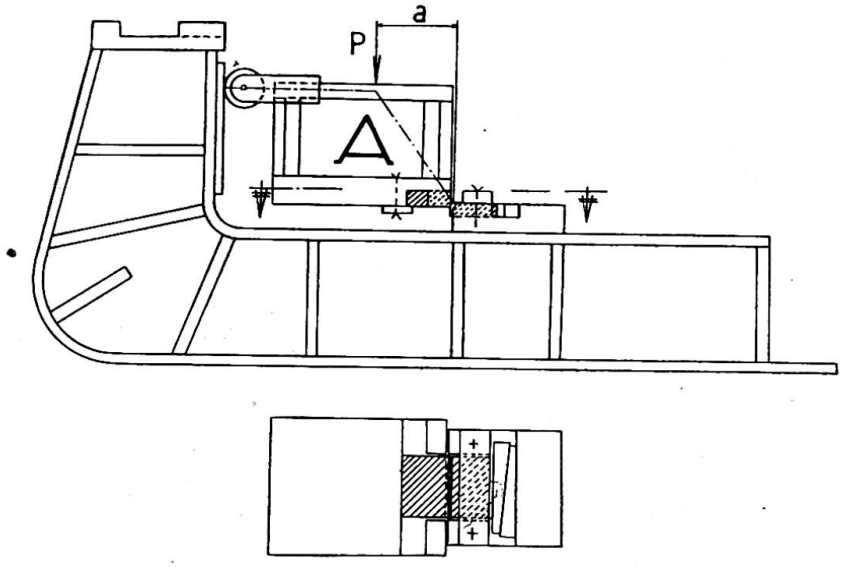

Fig. 1

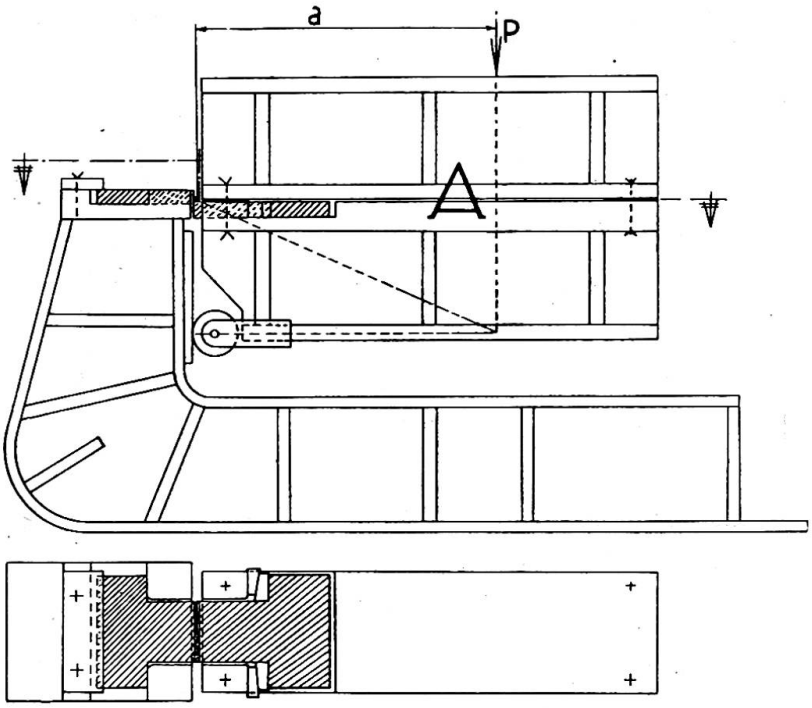

Fig. 2

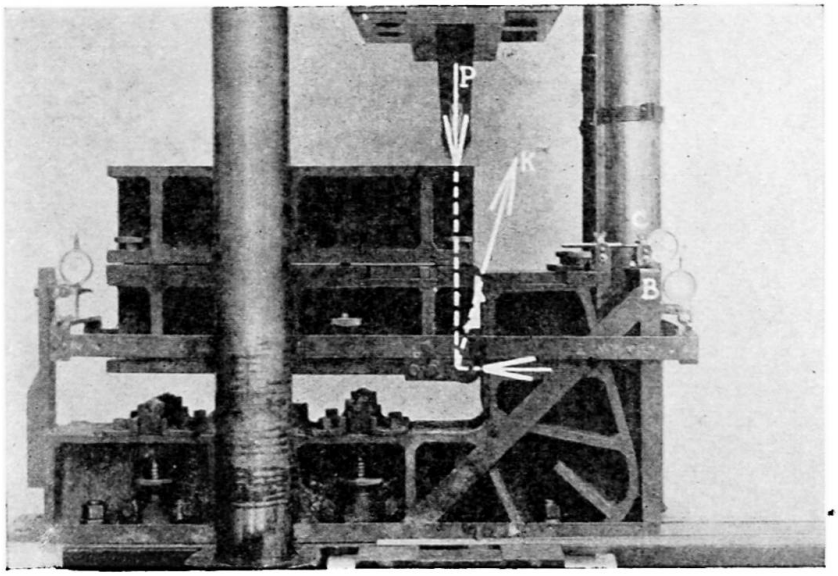

Fig. 3

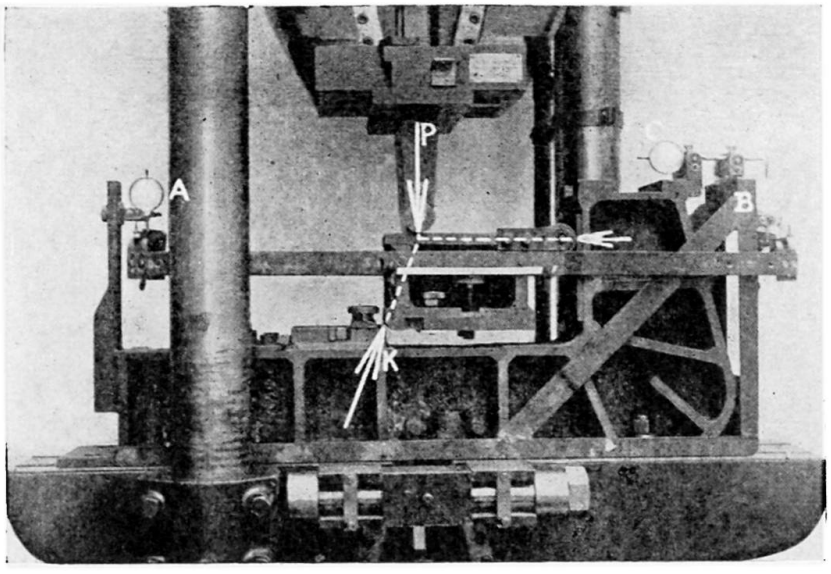

Fig. 4

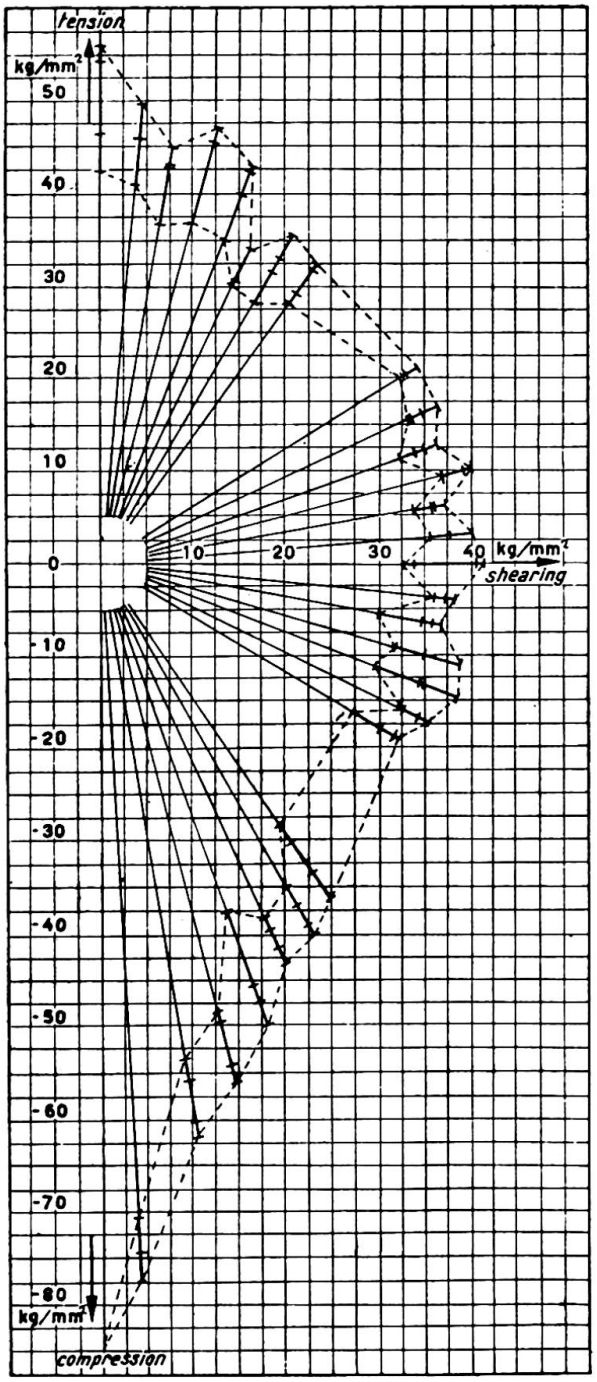
tension
kg/mm²
50
40
30
20
10
0
-10
-20
-30
-40
-50
-60
-70
-80
kg/mm²
compression
10
20
30
40 kg/mm²
shearing

Fig. 5

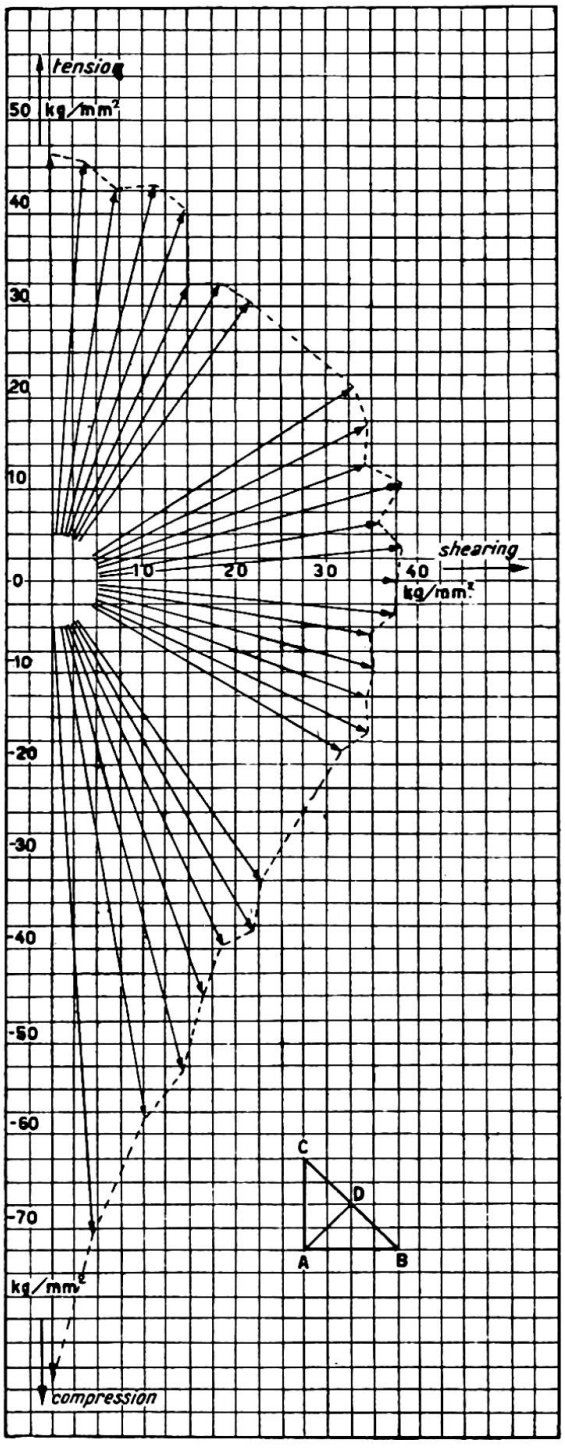
tension
50 kg/mm²
40
30
20
10
0
-10
-20
-30
-40
-50
-60
-70
kg/mm²
compression
10
20
30
40
kg/mm²
shearing
C
D
A
B

Fig. 6

as identical with the fracture section in every case; on the contrary this occurred only a few times.

Fig. 7 shows the relation between the angle of fracture β and the angle of force α,

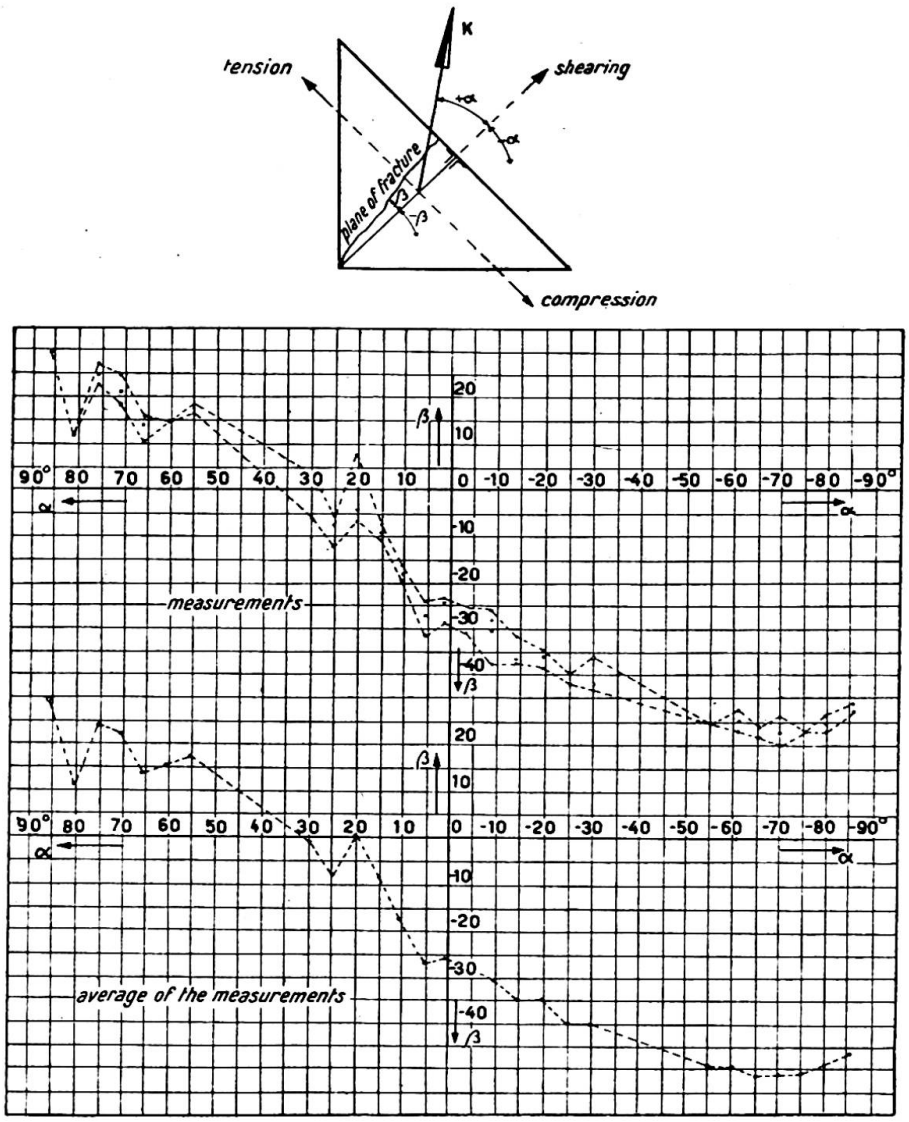

Fig. 7

whilst fig. 8 gives the same concerning the angle γ between the plane of fracture and the direction of force to the angle of force α.

THEORY OF THE FORMATION OF CRACKS

The most striking result obtained was the ratio between the rupture stresses in the case of pure tensile stress in comparison with those occurring in the case of pure shearing stress. This ratio showed a considerable deviation from the expected value of 1·67. For in the case under consideration, the ratio $\frac{\sigma_{tensile\ stress}}{\sigma_{shearing\ stress}}$ had a value of 1·24. This value again strongly supported the fracture hypothesis of Mariotte-

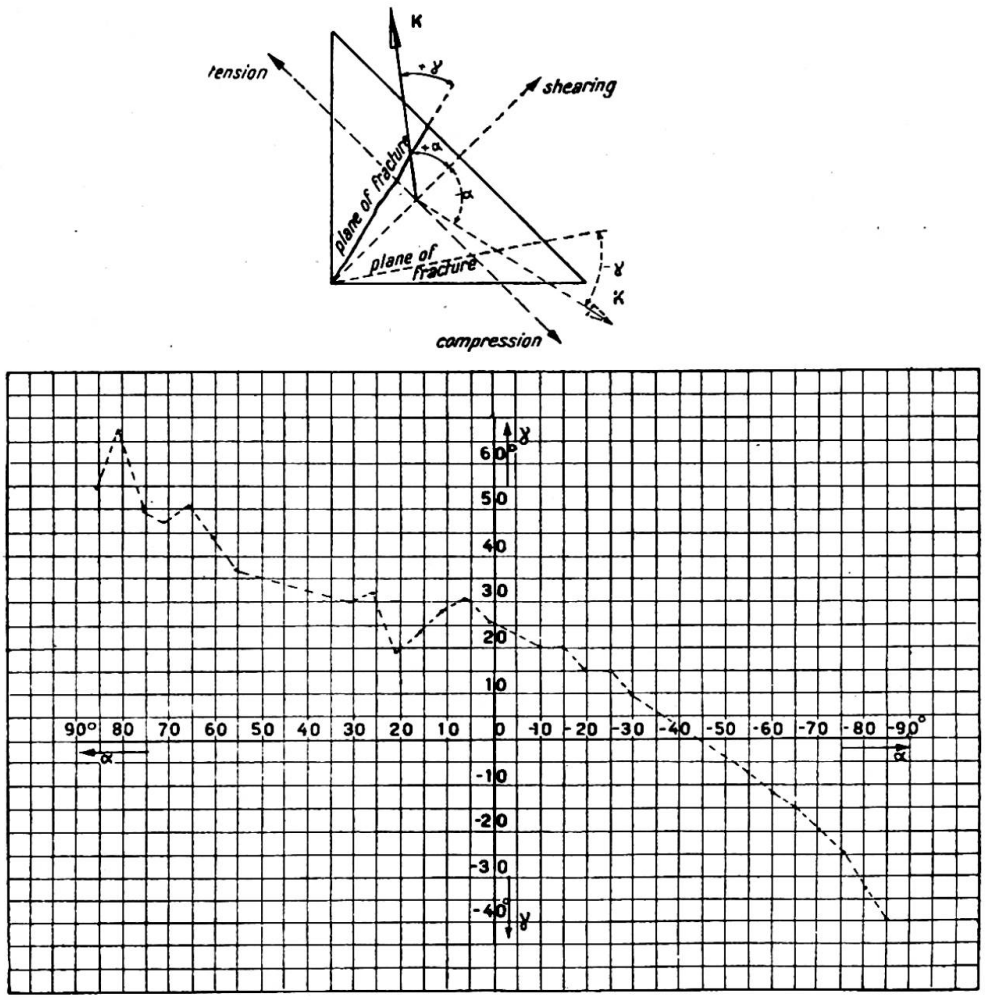

Fig. 8

Poncelet which had long been rejected. In view of the fact that the Fracture Research Committee (and particularly Prof. Dr. Ir. F. K. Th. van Iterson) are inclined on the strength of numerous experiments to reinstate this former theory, it seems reasonable to apply this old theory in the present case on the basis of the established ratio of 1·24.

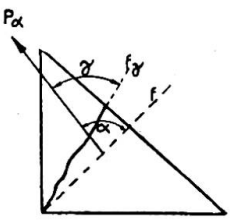

Fig. 9

The only assumption made is a uniform distribution of stress over the section (see fig. 9).

Applying the hypothesis of Poncelet, which is formulated thus:

$$\rho_i=\rho_x-m\,(\rho_y+\rho_z)$$

we find after substituting this in the case of plane stress condition:

$$\rho_i=\sigma_\alpha \cos(\alpha-\gamma_1)\left[\frac{1-m}{2}\sin\gamma_1+\frac{1+m}{2}\sqrt{1+3\cos^2\gamma_1}\right]$$

or

$$\sigma_\alpha=\frac{\rho_i}{\cos(\alpha-\gamma_1)\left[\frac{1-m}{2}\sin\gamma_1+\frac{1+m}{2}\sqrt{1+3\cos^2\gamma_1}\right]}=\Phi_1\rho_i$$

This latter relation is valid for the fibres at the two ends of the weld fillet. The

fibres in the middle part are more predominantly subjected to a plane *deformation condition.*

According to the mathematical theory of elasticity, the stress in the z direction is given by the formula:

$$\sigma_z = m\,(\sigma_x + \sigma_y)$$

Introducing this third stress condition gives:

$$\rho_i = \sigma_\alpha \cos(\alpha-\gamma_2)\cdot\left[\frac{1-m-2m^2}{2}\sin\gamma_2 + \frac{1+m}{2}\sqrt{1+3\cos^2\gamma_2}\right]$$

or

$$\sigma_\alpha = \frac{\rho_i}{\cos(\alpha-\gamma_2)\left[\frac{1-m-2m^2}{2}\sin\gamma_2 + \frac{1+m}{2}\sqrt{1+3\cos^2\gamma_2}\right]} \Phi_2\rho_i$$

In the values Φ_1 and Φ_2, the value γ is still unknown. This value must, of course, be determined in such a way that σ_α is a minimum. In view of the transcendent relationships it proves best to apply the method of trial and error. In varying the value of m, the closest possible correspondence with the ratio $\frac{\sigma_{tensile\ stress}}{\sigma_{shearing\ stress}}$ found by the tests is obtained.

The ultimate result is shown in the following tables.

Condition of plane stress (fibres at ends of the fillet) $m_1 = 0{\cdot}22$

α	0°	+15°	+30°	+45°	+60°	+75°	+90°
γ_1	+10°	+20°	+27½°	+35°	+45°	+55°	+70°
Φ_1	0·798	0·773	0·771	0·793	0·836	0·902	0·989

Condition of plane deformation (fibres in middle part) $m_2 = 0{\cdot}18$

α	0°	+15°	+30°	+45°	+60°	+75°	+90°
γ_2	+10°	+20°	+27½°	+35°	+45°	+55°	+70°
Φ_2	0·824	0·799	0·797	0·819	0·863	0·932	1·022

The values found for γ_1 and γ_2 have been rounded off. It will be seen from these numerical data that rupture tends to begin at the two ends of the fillet, where plane stress condition rules. In figs. 10 and 11 the result is plotted in comparison with the results of measurement and it is established that, *in the region of tensile stress*, there is a surprising agreement between theory and practice.

In the region of compressive stress these values show larger deviations, beginning at about the region of pure shearing stress, mainly concerning the angle of rupture.

The series of tests described was supplemented afterwards by four series of similar tests carried out on ten test pieces of the form shown in the sketches below.

Half the number of test pieces in the welding series A and B were finished as accurately as possible to the prescribed size, while the other half were left unfinished. Thus, the test pieces Aa–Ae and Ba–Be were left unfinished, whilst the test pieces Af–Ak and Bf–Bk were finished as accurately as possible. However, before the test pieces were loaded until rupture, the dimensions of the neck sections were measured as accurately as possible. The results of the tests are given in the following tables.

The calculated oblique stresses σ_α, found by dividing the observed breaking force by the area of the neck section, are given by: P/f_t. These latter stresses are averaged arithmetically.

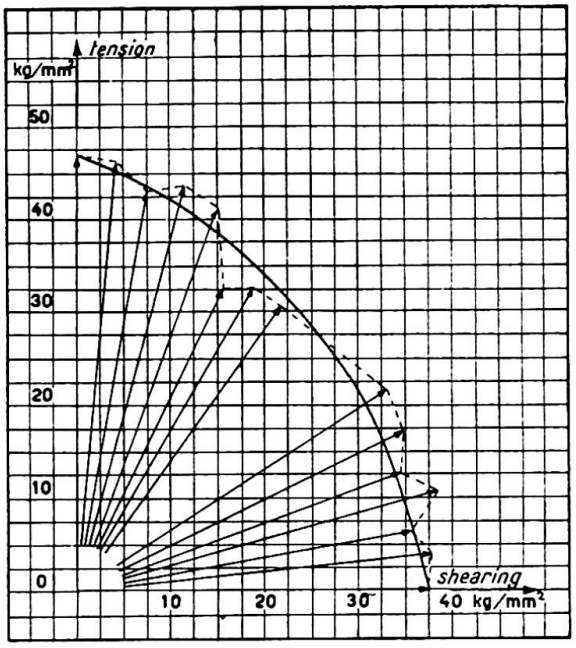

Fig. 10

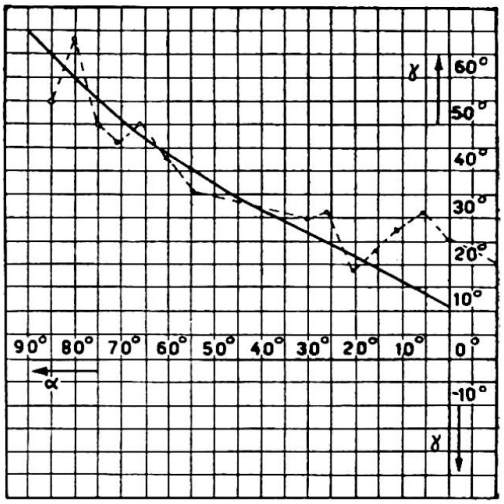

Fig. 11

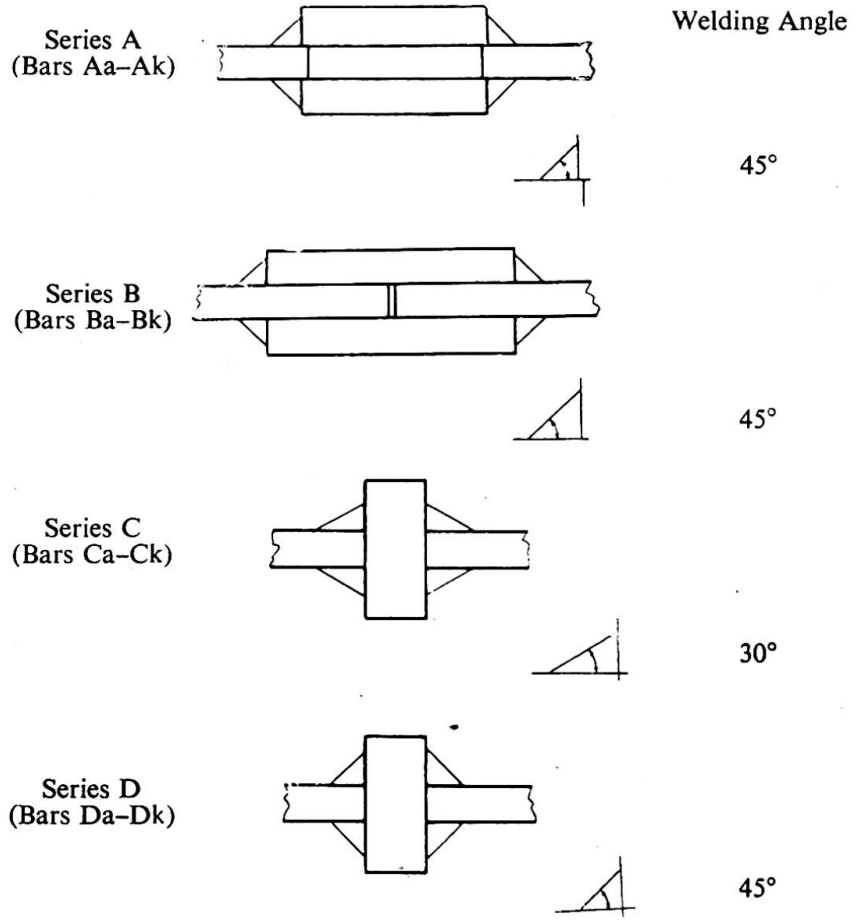

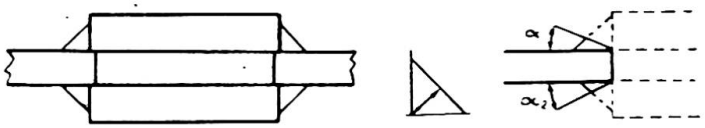

Type | Height of Weld | Angle of fracture

Type A		Of the two neck sections: Average height of weld in mm.	Width in mm.	Total area f_t	P Rupture force in metric tons	σ_a in kg./mm.^{2}	Angle of fracture: α_1	α_2
unfinished	Aa	~8·8	83·9	1476·6	36·5	24·71	33°	36°
	Ab	~9·0	85·9	1546·2	35·7	23·08	36°	—
	Ac	~4·8	79·6	764·2	25·8	33·76	43°	40°
	Ad	~8·2	76·8	1259·5	33·6	26·67	73°	36°
	Ae	~7·5	84·8	1272·0	41·7	32·78	27°	30°
				Average value:		28·2		
finished	Af	4·2	77·6	651·84	24·6	37·73	34°	36°
	Ag	3·8	79·6	604·96	29·6	48·92	28°	23°
	Ah	4·2	79·6	668·64	26·9	40·23	39°	—
	Aj	4·2	85·9	721·56	32·2	44·62	40°	—
	Ak	3·9	86·1	671·58	33·1	49·28	45°	—
				Average value:		44·16		

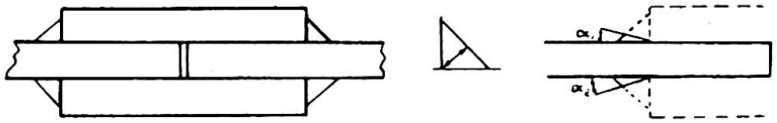

Type | Height of weld | Angle of fracture

Type B		Of the two neck sections: Average height of weld in mm.	Width in mm.	Total area f_t	P Rupture force in metric tons	σ_a in kg./mm.^{2}	Angle of fracture: α_1	α_2
unfinished	Ba	~7·0	82·9	1160·6	49·7	42·82	36°	30°
	Bb	~7·0	80·1	1121·4	54·5	48·59	73°	—
	Bc	~7·0	83·1	1163·4	50·0	42·97	30°	—
	Bd	~4·2	84·5	709·8	44·5	62·69	32°	36°
	Be	~6·0	84·1	1009·2	52·5	52·02	33°	—
				Average value:		49·82		
finished	Bf	3·8	84·6	642·96	46·5	73·32	31°	31°
	Bg	3·7	84·8	627·52	45·0	71·71	43°	19°
	Bh	3·8	84·4	641·44	46·7	72·80	21°	26°
	Bj	4·0	82·1	656·80	42·0	63·94	28°	27°
	Bk	3·4	85·8	583·44	46·0	78·84	17°	43°
				Average value:		71·92		

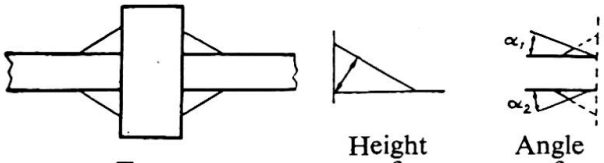

Type — Height of weld — Angle of fracture

Type C		Of the two neck sections			P Rupture force in metric tons	σ_a in kg./mm.²	Angle of fracture	
		Average height of weld in mm.	Width in mm.	Total area f_t			α_1	α_2
finished	Ca	3·8	77·2	586·7	38·7	65·96	32°	35°
	Cb	4·0	81·0	648·0	35·5	54·79	37°	40°
	Cc	4·0	78·6	628·8	36·0	57·25	34°	42°
	Cd	3·9	73·8	575·6	32·2	55·94	40°	42°
	Ce	3·8	79·9	607·2	36·2	59·61	40°	38°
	Cf	4·2	75·1	630·8	37·6	59·60	38°	45°
	Cg	4·1	76·1	624·0	31·2	49·99	30°	25°
	Ch	4·0	74·8	598·4	35·4	59·15	33°	42°
	Cj	4·1	81·0	664·2	34·7	52·24	36°	20°
	Ck	3·8	77·0	585·2	33·7	57·58	28°	20°
				Average value:		57·2		

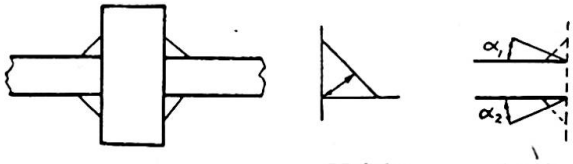

Type — Height of weld — Angle of fracture

Type D		Of the two neck sections			P Rupture force in metric tons	σ_a in kg./mm.²	Angle of fracture	
		Average height of weld in mm.	Width in mm.	Total area f_t			α_1	α_2
unfinished	Da	~5·2	83·2	865·3	38·1	44·03	33°	27°
finished	Db	3·8	80·7	613·3	30·5	49·73	20°	20°
	Dc	4·2	76·5	642·6	28·7	44·66	23°	29°
	Dd	3·9	80·7	629·5	32·7	51·94	36°	28°
	De	4·0	77·9	623·2	31·6	50·70	25°	27°
	Df	4·0	79·6	636·8	31·4	49·30	30°	35°
	Dg	4·0	81·5	652·0	30·0	46·01	36°	23°
	Dh	4·0	80·0	640·0	28·0	43·75	24°	33°
	Dj	3·9	76·3	595·1	33·8	56·79	29°	29°
	Dk	3·9	80·8	630·2	31·8	50·45	39°	28°
				Average value:		48·74		

The results of series A and B are notable. The unfinished test pieces, having a larger neck section than the finished specimens, show definitely lower rupture stresses than the finished specimens with smaller neck sections. This can only be due to unequal distribution of stress in the end fillet weld. It could not have been due to the finishing of the test pieces, as the finished test piece Bd, which happened to turn out somewhat small, likewise shows a conspicuously high average rupture stress in comparison with the other finished specimens.

This peculiarity may be accounted for as follows. Under the given condition of stress, an end fillet weld, in the case of a very small neck section, can be represented in a simplified scheme outlined below (fig. 12).

A somewhat thicker weld may be represented by fig. 13 and a still thicker one by fig. 14.

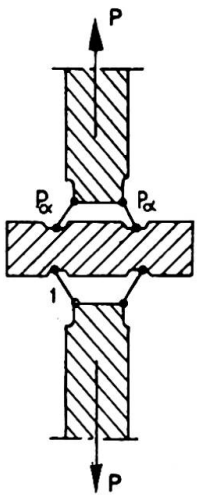

Fig. 12

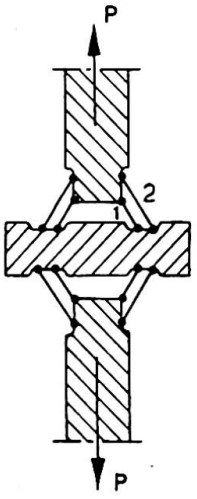

Fig. 13

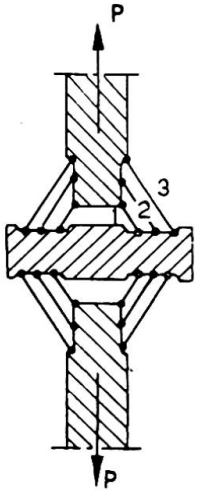

Fig. 14

It is assumed that a small portion of the material in the adjoining sections will yield with the rest. The non-yielding parts of these adjoining sections may then be regarded as having $\sim$ rigidity.

Lastly fig. 15 gives the $\sigma-\epsilon$ diagram for material that is prevented from contracting crosswise.

Considering fig. 12 the force P will now be resolved into the two components P_α whereby bars 1 are subjected after yielding to a pure, uniformly distributed normal stress. At the moment of rupture there exists in these bars a rupture stress σ_p corresponding to the rupture elongation ϵ_1. This stress σ_p in bars 1 is correlated to the force P in the drawbench.

Considering the case in fig. 13, the moment again is reached at which the rupture stress σ_p (or the rupture elongation ϵ_p) exists. However, σ_p does not exist at that moment in bars 2. This is clear by the fact that on account of the bigger length of the bars 2 there is a considerably lower specific elongation in these bars (depending on the ratio of the lengths). When the specific elongation in bars 1 is again of the same value as in the previous case, viz. ϵ_1, its value in bars 2 is ϵ_2, corresponding to a stress $\sigma_{\alpha p}$. However, rupture is defined by bars 1, which crack at the moment when σ_p (or ϵ_1) is reached, as a result of which bars 2 suddenly become overstrained and likewise crack without causing any further increase of force in the drawing machine.

The force in the drawing machine being P in the first case causing an average

stress σ_p, this will be in the second case $P+\alpha P$, (where $\alpha<1$), resulting in an average stress $\sigma_{average}=\frac{1+\alpha}{2}\sigma_p$, which is smaller than σ_p. Reasoning analogously for the case given in fig. 14, the average stress value is found to be:

$$\sigma_{average}=\frac{1+\alpha+\beta}{3}\sigma_p<\frac{1+\alpha}{2}\sigma_p<\sigma_p$$

in which $\beta<\alpha<1$. In this way the simplified scheme clearly shows that there cannot be a uniformly distributed stress in the cross-section at the moment of rupture. It also appears that the *elongation* at rupture must be a decisive factor, a fact which again supports the rupture hypothesis of Mariotte-Poncelet in this case of stress.

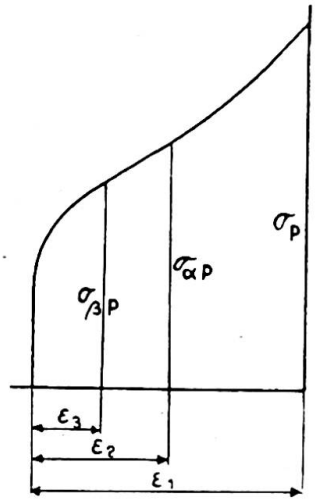

Fig. 15

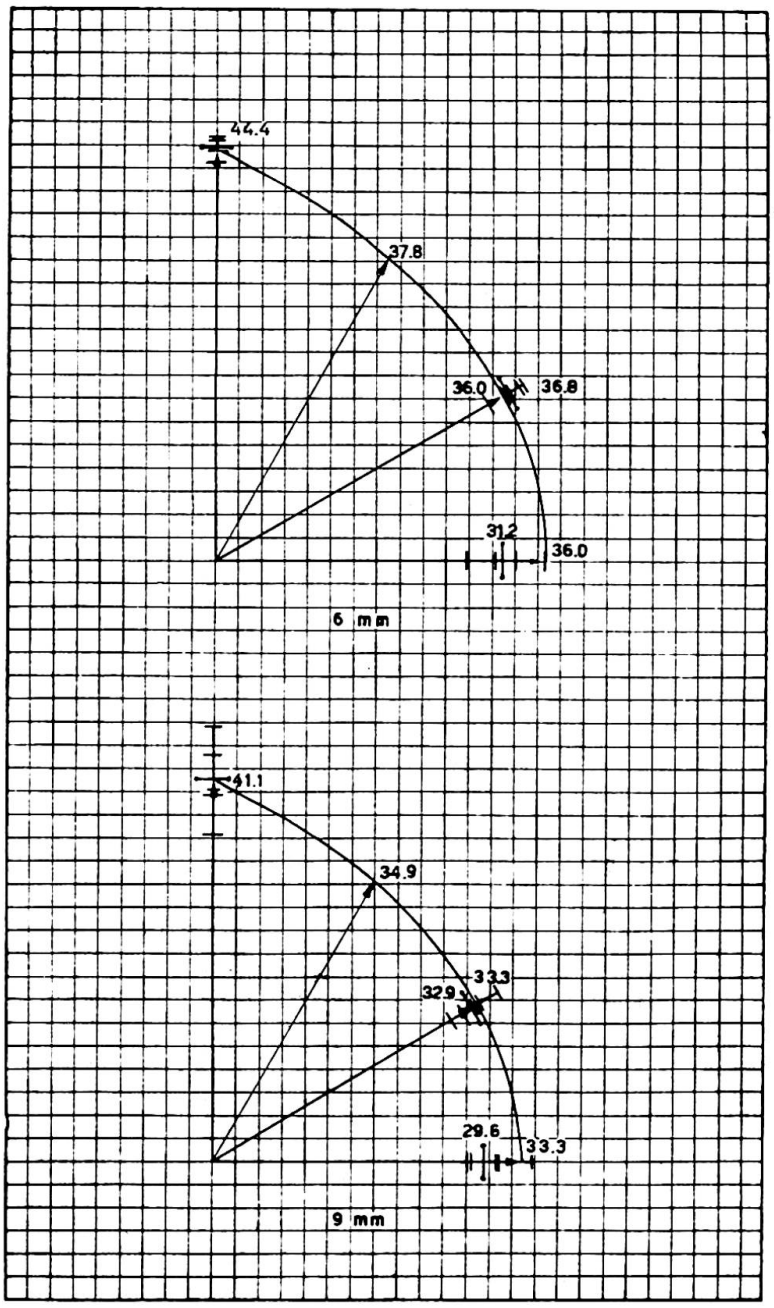

Fig. 16(a)

As a consequence of the test results of the second series of test pieces, which showed a diminution in rupture stress measured on the neck section of the weld, a third series of tests on end fillet welds followed, for which purpose the original installation first described was used. The object in view in this third series was to ascertain the effect of the weld height on the average rupture stress under various stress conditions to which the weld may be subjected. Altogether 45 test pieces were provided for this test series, 15 of which were used for each of the following cases of elasticity:

(1) pure tensile stress,
(2) pure shearing stress,
(3) a combination of tensile and shearing stress

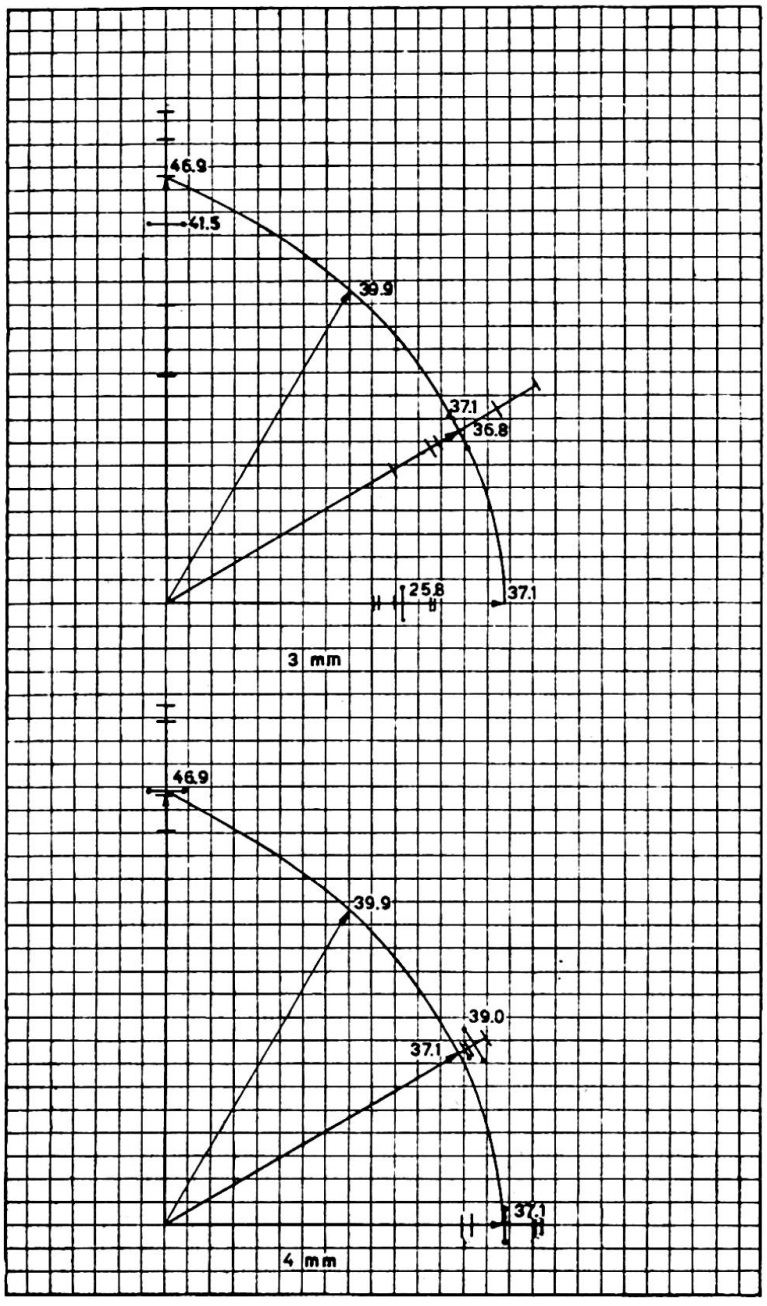

Fig. 16(b)

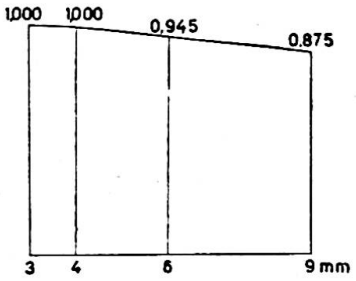

Fig. 17

in which the line of force shows a deviation of 30° from the pure shearing position. In each of these cases the 15 test pieces used consisted of groups having a height of 3 mm., 6 mm. and 9 mm. respectively.

The test results are given in the accompaning polar diagrams, in which the average results are indicated by ●—● and the test results by a cross-line (figs. 16(*a*) and 16(*b*)).

For the sake of brevity reference is made to these diagrams.

With the exception of the test results of the test pieces having 3 mm. weld height, which show very wide dispersions, the same tendency is observable in every case, viz. that the average results for pure shearing stress are considerably higher than would be expected according to the rupture hypothesis of Huber-Hencky.

The wide divergencies found in the case of the 3-mm. welds are not surprising, as errors in welding manifest themselves to a much greater extent in these small thicknesses.

It is again found in these cases that the rupture hypothesis of Mariotte-Poncelet is the one that gives the closest accordance with the test results.

Also reproduced in the diagrams are the ideal characteristics on the basis of the rupture theory of Mariotte-Poncelet, those for 3 mm. and 4 mm. having been smoothed out. From these characteristics the average reduction factor as a function of the weld height may be concluded to be as shown in the following graph. The curve in the region under consideration is found to be almost linear (fig. 17).

Summary

This article deals with the investigation of the static strength of end fillet welds under various conditions of stress. A large number of test pieces were subjected to tensile or to compressive stress, in such a way that the direction of action of the applied force showed a varying angle α with the normal to the narrow part of the cross-section of the weld. This was achieved by means of a testing apparatus specially designed for the purpose.

Furthermore, the effect produced by different weld heights was also examined on the same apparatus.

Similar tests in completion of this series were carried out on end fillet welds of various forms occurring in practice.

From the entire series of tests it is evident that the rupture hypothesis which corresponds most closely with the test results in regard to both breaking strength as well as angle of rupture is the rupture hypothesis of Poncelet which has long been abandoned. This result is fully in accordance with the conclusion of Prof. van Iterson, who arrived at his results on the basis of other tests.

In addition it is found that the average rupture strength diminishes as the weld height increases. This latter phenomenon can be proved theoretically.

In these experiments special emphasis was laid on the question of the divergency of the test results; accordingly a large number of test pieces were subjected to test.

Résumé

L'auteur expose des essais de résistance statique de soudures angulaires frontales, sous différentes conditions de charge. Un grand nombre de pièces a été soumis suivant le cas, à un effort de traction ou de compression dont la direction forme un angle α avec la normale à la coupe transversale de la partie étroite de la soudure. On a utilisé ici un appareil d'essai spécialement conçu.

On a ensuite étudié sur le même appareil l'influence de différentes épaisseurs de soudure.

Cette série d'essais a été enfin complétée par l'examen de quelques formes de soudures angulaires frontales qui se présentent en pratique.

Cette série d'essais a démontré qu'entre les diverses hypothèses de rupture, celle de Poncelet, considérée depuis longtemps comme démodée, correspond le mieux aux résultats des essais, tant pour l'angle de rupture que pour la charge de rupture. Cette conclusion s'accorde tout-à-fait avec les faits constatés par le professeur van Iterson d'après des résultats obtenus dans d'autres essais.

En outre, il a été constaté que la charge de rupture diminue lorsque l'on augmente l'épaisseur de la soudure. Il est possible de donner une explication théorique de ce dernier phénomène.

Au cours des essais, on a fait porter particulièrement l'attention sur la divergence des résultats obtenus; c'est pourquoi on avait préparé un grand nombre d'eprouvettes.

Zusammenfassung

In der vorstehenden Abhandlung wird die statische Festigkeit von elektrisch geschweissten Stirnkehlnähten unter verschiedenen Beanspruchungsverhältnissen untersucht. Eine grosse Anzahl Probestücke wurde einer Zug- resp. Druckkraft unterworfen, derart, dass deren Wirkungslinie mit der Normalen zum engsten Schnitt der Schweissnaht einen variablen Winkel α bildete. Dies wurde mittels eines speziell hierfür entworfenen Prüfungsapparates erreicht.

Ferner wurde auf demselben Apparat der Einfluss verschiedener Schweissnahtdicken untersucht. Schliesslich wurde die Prüfungsserie mit einer Reihe in der Praxis vorkommender Stirnkehlnaht-Typen abgeschlossen.

Aus der ganzen Prüfung ergab sich, dass die schon lange als veraltet betrachtete Bruchhypothese von Poncelet sowohl bezüglich Bruchfestigkeit als auch bezüglich Bruchwinkel am besten mit den Prüfungsergebnissen übereinstimmt. Dieses Resultat bestätigt die Beobachtungen Prof. van Itersons, der seine Feststellungen auf andere Versuche gründete.

Ferner zeigte sich, dass bei zunehmender Schweissnahtdicke die mittlere Bruchspannung abnimmt, was auch theoretisch bewiesen werden kann.

Bei diesen Versuchen wurde der Streuung der Prüfungsergebnisse besondere Beachtung geschenkt; demgemäss wurde eine grosse Anzahl Probestücke untersucht.

Supplementary note

About 1930 theories were developed by Prof. Ir. N. C. Kist, which have led to the calculation methods standardised in the Netherlands Standards N 657 and in N 1017.

Prof. Kist based his ideas on experimental results of C. J. Jensen and the results of his own experiments.

It was inevitable that certain simplifications formed the basis for his considerations. On many of these suppositions well founded critique could be passed.

Moreover, the way in which Prof. Kist applied the results of his own tests and those of C. J. Jensen gave rise to many objections.

These two facts were the reasons for carrying on and enlarging the work of Prof. Kist. Under the direction of Prof. Ir. C. G. J. Vreedenburgh, professor at the Technical University, Delft, the above described tests were done as an extension of the work already done in this field.